320
Copy
RM L55K11

CONFIDENTIAL

NACA RM L55K11

NACA

CASE FILE
COPY

RESEARCH MEMORANDUM

EXPERIMENTAL INVESTIGATION AT HIGH SUBSONIC SPEED OF THE ROLLING STABILITY DERIVATIVES OF A COMPLETE MODEL HAVING A CLIPPED-DELTA WING AND A HIGH HORIZONTAL TAIL

By William C. Sleeman, Jr., and Albert G. Few, Jr.

Langley Aeronautical Laboratory
Langley Field, Va.

CLASSIFICATION CHANGED TO UNCLASSIFIED
AUTHORITY: NACA RESEARCH ABSTRACT NO. 122
EFFECTIVE DATE: NOVEMBER 8, 1957
WHL

CLASSIFIED DOCUMENT

This material contains information affecting the National Defense of the United States within the meaning of the espionage laws, Title 18, U.S.C., Secs. 793 and 794, the transmission or revelation of which in any manner to an unauthorized person is prohibited by law.

NATIONAL ADVISORY COMMITTEE
FOR AERONAUTICS

WASHINGTON

February 17, 1956

CONFIDENTIAL

NATIONAL ADVISORY COMMITTEE FOR AERONAUTICS

RESEARCH MEMORANDUM

EXPERIMENTAL INVESTIGATION AT HIGH SUBSONIC SPEED OF THE ROLLING STABILITY DERIVATIVES OF A COMPLETE MODEL HAVING A CLIPPED-DELTA WING AND A HIGH HORIZONTAL TAIL

By William C. Sleeman, Jr., and Albert G. Few, Jr.

SUMMARY

An investigation was conducted in the Langley high-speed 7- by 10-foot tunnel to determine the rolling stability derivatives of a complete model and its components over a Mach number range from 0.60 to 0.92 and an angle-of-attack range from 0° to a maximum of approximately 13° for the lower Mach numbers. The aspect-ratio-3 clipped-delta wing of the model was swept back 45° at the leading edge and had NACA 65A006 airfoil sections parallel to the free stream. The delta planform horizontal tail was swept back 45° at the leading edge and was located at the tip of a sweptback vertical tail approximately 65 percent of the wing semispan above the wing-chord plane.

Positive damping in roll was indicated for the model throughout the test Mach number and angle-of-attack range, although significant losses in damping occurred in going from moderate to high angles of attack. Addition of the tail surfaces to the wing-fuselage configuration had little overall effect on the damping in roll and gave negative increments of yawing moment due to rolling throughout the test angle-of-attack range above approximately 4°. Estimates of the rolling stability derivatives of the complete model at $M = 0.85$ indicated that these derivatives could be estimated with fairly good accuracy by use of existing procedures.

Wing-fuselage damping-in-roll characteristics at lifting conditions for the aspect-ratio-3 clipped-delta-wing model were slightly better than those for the parent aspect-ratio-4 delta-wing model throughout the test range of Mach number and angle of attack.

INTRODUCTION

Wind-tunnel results at high subsonic speeds pertaining to rolling-stability derivatives for lifting conditions have been obtained for a fairly wide range of wing plan forms (refs. 1 to 3). These derivatives were obtained on model configurations without tail surfaces and more experimental data have been needed to indicate the applicability of existing procedures based on low-speed results for estimating the tail contribution to rolling-stability derivatives. The present test results were obtained as part of a research program to determine the longitudinal, lateral, and rolling-stability characteristics of a general research model. Results presenting the static longitudinal stability of the model are given in reference 4. The clipped-delta wing of the model was of aspect ratio 3, taper ratio 0.143, and had NACA 65A006 airfoil sections. The leading edge of the wing and of the delta plan-form horizontal tail were swept back 45° and the horizontal tail was located at the tip of a swept vertical tail approximately 65-percent wing semispan above the wing chord plane. The model was tested in the Langley high-speed 7- by 10-foot tunnel over a Mach number range from 0.60 to 0.92 and an angle-of-attack range from 0° to a maximum of approximately 13°.

In addition to tests of the complete model, breakdown tests were made in order to determine the contribution of the tail surfaces to the rolling derivatives of the model with and without the wing. Test results for other models having both swept and unswept wings, which show contributions of the model components in addition to the complete model rolling derivatives, are presented in references 5 and 6.

COEFFICIENTS AND SYMBOLS

The results of this investigation are presented as standard NACA coefficients of forces and moments referred to the stability system of axes shown in figure 1. Moment coefficients are given with respect to the moment reference location shown in figure 2 (25-percent mean aerodynamic chord on the fuselage center line).

C_L lift coefficient, $\frac{\text{Lift}}{qS}$

C_l rolling-moment coefficient, $\frac{\text{Rolling moment}}{qSb}$

C_n yawing-moment coefficient, $\frac{\text{Yawing moment}}{qSb}$

C_Y lateral-force coefficient, $\frac{\text{Lateral force}}{qS}$

q dynamic pressure, $\frac{\rho V^2}{2}$, lb/sq ft

ρ air density, slugs/cu ft

V free-stream velocity, ft/sec

p rolling angular velocity, radians/sec

$pb/2V$ wing-tip helix angle, radians

M free-stream Mach number

α angle of attack, deg

S wing area, sq ft

b wing span, ft

$\bar{c}$ wing mean aerodynamic chord, ft

$\bar{c}_h$ horizontal tail mean aerodynamic chord, ft

$\bar{c}_v$ vertical tail mean aerodynamic chord, ft (based on area above root chord shown in fig. 2)

$$C_{l_p} = \frac{\partial C_l}{\partial \frac{pb}{2V}}$$

$$C_{n_p} = \frac{\partial C_n}{\partial \frac{pb}{2V}}$$

$$C_{Y_p} = \frac{\partial C_Y}{\partial \frac{pb}{2V}}$$

Configuration designations:

W	wing
F	fuselage
V	vertical tail
H	horizontal tail

MODEL AND APPARATUS

A drawing of the model with pertinent geometric characteristics is given as figure 2 and details of the fuselage geometry are given in figure 3. The model wing was of aspect ratio 3, taper ratio 0.143, and had a leading-edge sweep angle of 45°. The wing airfoil section was NACA 65A006 parallel to the free-stream direction. The aspect-ratio-4 delta plan-form horizontal tail had 45° leading-edge sweep and was located at the tip of the vertical tail approximately 65 percent of the wing semispan above the wing chord plane. The vertical tail was swept back 28° at the quarter-chord line. Other details of the model geometry are given in table I. Both the horizontal and vertical tails had NACA 65A006 airfoil sections and were constructed of fiberglas and plastic, reinforced with a steel spar. The wing was constructed of 2024-T (formerly 24S-T) aluminum alloy.

The model was tested under conditions of steady rolling on the forced-roll sting support shown schematically in figure 4. For these tests, the model was mounted on a six-component internal strain-gage balance and was rotated about the X-axis of the stability axes. Electrical signals from the strain-gage balance were transmitted to the data-recording equipment by means of wire leads, slip rings, and brushes (fig. 4). The model angle of attack was changed by use of various offset sting adapters (fig. 4) which were designed to allow the model to rotate about the moment reference center at each angle of attack. Further details of the forced-roll testing technique can be found in reference 5.

TESTS AND RESULTS

Test conditions.- Tests were conducted in the Langley high-speed 7- by 10-foot tunnel over a Mach number range from 0.60 to 0.92 and through an angle-of-attack range from 0° to a maximum of approximately 13°. Test results were also obtained at $M = 0.95$ for the zero-lift

condition only. For most of the tests, four positive and four negative values of $pb/2V$ were obtained at each Mach number and angle of attack. The variation with Mach number of the maximum test value of wing-tip helix angle $pb/2V$ and mean test Reynolds number based on the wing mean aerodynamic chord are presented in figure 5.

Corrections.- Jet-boundary corrections to the angle of attack were determined from the usual static corrections presented in reference 7. Blockage corrections applied to the Mach number and dynamic pressure were determined from reference 8. The model angle of attack has also been corrected for deflection of the model and support system under load.

The deflections of the support system under load combined with any initial displacement of the mass center of gravity of the model from the roll axis introduced centrifugal forces and moments when the model was rotated. Corrections for these forces and moments have been applied to the data.

Corrections for jet-boundary effects on rotary derivatives were not applied inasmuch as these corrections have been found to be negligible for models comparable in size to the present model. Corrections for wing distortion and sting support tares have not been applied to the data; however, these corrections are believed to be small.

Results.- The basic results of this investigation were obtained as variations of forces and moments with wing-tip helix angle; inasmuch as these variations were linear in most cases, only the derivatives are presented herein. For convenience, some of the static-lift curves obtained from reference 4 are given in figure 6.

Test results presenting the rolling-stability derivatives of the complete model and also showing effects of the addition of the vertical tail and the horizontal tail are given in figure 7. Rotary derivatives obtained with the wing removed, which show effects of the horizontal tail, are presented in figure 8. Rolling derivatives for the present clipped-delta wing-fuselage configuration at $M = 0.85$ are compared in figure 9 with those of the aspect-ratio-4 delta wing from which the present wing was derived. Additional comparisons between results for the clipped-delta wing and parent delta wing are given in figures 10 and 11. A comparison of experimental and estimated rolling derivatives through the angle-of-attack range at $M = 0.85$ for the wing-fuselage configuration, the tail contribution, and the complete model is presented in figures 12 to 15.

DISCUSSION

Experimental Derivatives

Damping in roll.- The experimental damping in roll obtained for all the wing-on configurations tested (fig. 7) indicated similar trends with angle of attack for the test range of Mach number. The damping-in-roll derivative C_{l_p} increased as the angle of attack increased from 0° to approximately 3° and then decreased appreciably as the highest test angle of attack was approached. No outstanding differences in damping in roll were apparent as a result of addition of the tail surfaces although addition of each of the tail surfaces increased the damping somewhat at the lower angles of attack.

Effects of clipping the tips of an aspect-ratio-4 delta wing (ref. 2) to the aspect-ratio-3 wing of the present investigation are shown in figure 9 for the wing-fuselage configuration at Mach number 0.85. There was not much difference in the damping in roll at 0° angle of attack for the clipped-delta and basic-delta wing; however, the increase in damping at low angles of attack for the clipped delta was not evident for the aspect-ratio-4 delta wing. Above an angle of attack of approximately 4°, the variation of damping with angle of attack was about the same for the two wings; however, the clipped delta provided more damping throughout most of the angle-of-attack range tested.

The aforementioned losses in damping at lifting conditions for the aspect-ratio-4 delta wing and the present wing are related to lift coefficient and Mach number in figure 10. The solid and dashed lines in figure 10 indicate combinations of lift coefficient and Mach number for which the damping in roll for lifting conditions has decreased to one-half the initial damping value at zero lift. The dotted line indicates the maximum lift coefficients and corresponding Mach numbers obtained in the present tests. A comparison of results for the aspect-ratio-4 delta wing and the aspect-ratio-3 clipped-delta wing indicates that the clipped-delta wing configuration attained lift coefficients about 12 percent higher than the aspect-ratio-4 delta wing for the damping to decrease to one-half the zero lift value. Inasmuch as the damping values at zero lift were not appreciably different for the two wings, it would appear that the damping-in-roll characteristics of the clipped-delta wing were slightly better than the parent aspect-ratio-4 delta wing for Mach numbers up to $M = 0.90$.

Yawing moment and lateral force due to rolling.- The yawing moment due to the rolling derivative C_{n_p} for the complete-model configuration (fig. 7) was positive for angles of attack up to approximately 4°; above

this angle, negative values of C_{n_p} occurred which increased with increasing angle of attack. A comparison of the tail-on and tail-off curves of figure 7 shows that the tail contribution to C_{n_p} for the complete model was negative at angles of attack above approximately 4°, whereas addition of the tail surfaces to the wing-off configuration (fig. 8) gave positive increments of C_{n_p} for angles of attack up to 12° (assuming negligible values of rolling derivatives for the fuselage alone). This difference in tail contribution with and without the wing is due to the effect of wing sidewash due to roll which is discussed in reference 9.

The lateral-force derivative C_{Y_p} for the complete model was positive throughout the test angle-of-attack range above about 2°. Results for the wing-fuselage configuration indicate rather large negative values of C_{Y_p} at the highest test angle of attack, particularly at $M = 0.60$ and $M = 0.90$ (fig. 7). Based on past experience, these large negative values of C_{Y_p} were not expected and from a comparison with the aspect-ratio-4 delta wing of reference 2, for which only quite small values of C_{Y_p} were obtained at high angles of attack. (See fig. 9.) The experimental results of reference 10 indicate, however, that the rolling derivative C_{Y_p} can be appreciably influenced by fuselage size for a mid-wing arrangement having a 60° delta wing. Inasmuch as different fuselages were used for the aspect-ratio-4 delta wing and the present clipped-delta wing, some of the discrepancy in C_{Y_p} shown in figure 9 could be associated with effects of the fuselage differences.

Estimated Derivatives

Wing fuselage.- A comparison of the estimated and experimental variation of damping in roll with Mach number for the zero-lift condition is presented in figure 11. Estimated values were obtained from reference 11 using the indicated plan-form transformation to account for compressibility effects. The agreement between experimental and estimated damping in roll at zero lift was not quite as good as would be expected from past experience and was considerably less than would be expected from the excellent agreement shown between estimates and experiment for the aspect-ratio-4 delta wing (fig. 11). The close agreement of experimental results at zero lift for the aspect-ratio-4 delta wing and the aspect-ratio-3 clipped-delta wing appears reasonable inasmuch as the relative area removed in clipping the tips of the delta wing was

very small. This agreement for the two wings was also indicated at low speed for the wing-alone configuration. (See ref. 12.)

A comparison of experimental and estimated rolling stability derivatives through the test angle-of-attack range for a Mach number of 0.85 is given in figure 12. Estimated damping in roll was obtained by correcting the zero-lift value from reference 11 in accordance with the effects of angle of attack as indicated in reference 13, using static lift-curve slope ratios and drag data from reference 4. The predicted trends with angle of attack are in fairly good agreement with experimental trends although the experimental changes with angle of attack were much more pronounced than the estimated changes. The agreement between values of the damping as estimated and obtained experimentally was only fair and was approximately the same as the agreement shown in reference 2 for the aspect-ratio-4 delta wing when wing lift-slope ratios were used in the estimates. As pointed out in reference 2, the use of wing-root bending-moment slopes rather than lift slopes to account for nonpotential effects would be expected to give more accurate estimates of C_{l_p} for lifting conditions.

Estimated values of yawing moment due to rolling are compared with experimental results in figure 12. The estimates were obtained by applying the method outlined in reference 1 in which the potential-flow value determined from reference 11 was corrected for Mach number effects by using the relationships of reference 14, and for nonpotential effects by using experimental lift and drag data of reference 4 and estimated C_{l_p}. Estimates of C_{n_p} for the wing-fuselage configuration are in good agreement with experiment up to about 8° angle of attack. At higher angles of attack the negative values of C_{n_p} indicated by experiment did not appear in the estimates. The differences between estimated and experimental values of C_{n_p} were probably not due to the use of theoretical rather than experimental values of $C_{l_p} \tan \alpha$ because when experimental $C_{l_p} \tan \alpha$ was used, the C_{n_p} estimates deviated only slightly from those shown in figure 12. It is possible that a fuselage effect, not accounted for in the estimates, could cause the experimental results to differ from estimated C_{n_p}. The lateral-force derivative C_{Y_p} was estimated by the method given in reference 2 using values obtained from references 14 and 15. The values and trends with angle of attack shown by the estimated results are in good agreement with experiment up to about 9° angle of attack. In the higher angle-of-attack range, experimental values increased considerably in the negative direction as observed previously, whereas the estimates showed slightly decreasing values.

Tail contribution.- Estimates of the tail contribution to the rolling-stability derivatives of the model are compared with experimental results in figure 13 for 0.85 Mach number. Estimates were made by use of the procedure outlined in reference 16 and using the wing sidewash estimates of reference 9. Lift-curve slopes for the vertical tail in the presence of the horizontal tail through the angle-of-attack range were obtained from unpublished static-force data.

The small experimental contribution of the tail surfaces to C_{l_p} with the wing on was comparable in magnitude to other configurations (refs. 5 and 6) and could be estimated with reasonable accuracy. The tail contribution to C_{l_p} would be expected to be small because the rotating flow field behind the wing would reduce even further the relatively small direct damping contribution of the horizontal tail, and any vertical-tail contribution at 0° angle of attack would diminish as the load center of the vertical tail approached the rolling-moment reference axis at the higher angles.

The estimated contribution of the tail surfaces to the yawing-moment derivative for the wing-on configuration (fig. 13) was in fairly good agreement with experiment throughout the test angle-of-attack range; however, for the wing-off configuration, good agreement with experiment was not obtained particularly at low angles of attack. Causes for the differences between estimates and experiment for the wing-off configuration at low angles of attack are not apparent; however, these differences are consistent with the lateral-force derivatives which were also underestimated at the lowest angles but were in good agreement at moderate and high angles. The fairly large effect of wing sidewash on the tail contribution to both yawing moment and lateral force due to roll is indicated in both the estimates and experimental results of figure 13. Estimated wing sidewash effects were somewhat less than those obtained experimentally.

There was a rather large difference in experimental and estimated tail contribution to C_{Y_p} for the wing-on configuration at high angles of attack, and part of this difference may be associated with the previously mentioned large negative experimental values obtained for the tail-off configuration.

Inasmuch as the estimated horizontal-tail contribution to the rolling derivatives was very small, only the experimental contribution is presented in figure 14. Experimental increments in the rolling derivatives due to addition of the horizontal tail generally affected the test results in a manner that would be expected from an increase in the vertical-tail lifting effectiveness.

Complete model.- A comparison of estimated and experimental rolling-stability derivatives for the complete model at 0.85 Mach number is presented in figure 15. The general overall agreement between estimates and experiment was fairly good throughout the test angle-of-attack range. Estimates of the damping in roll showed a smaller variation with angle of attack than experiment as was indicated for the wing-fuselage configuration. Estimates of the other rolling derivatives C_{n_p} and C_{Y_p} were in good agreement with experiment at low and moderate angles of attack; however, at the higher angles, the magnitude of the estimated values was somewhat smaller than for the experimental values.

A comparison of estimated and experimental rolling-stability derivatives for the tail-off and complete-model configurations (figs. 12 and 15) would indicate (with the possible exception of C_{Y_p} at high angles of attack) that the same general discrepancies occur for both configurations. It would appear, therefore, that a large part of the disagreement between experiment and estimates for the complete model can be attributed to estimates for the wing-fuselage configuration rather than to estimates of the tail contribution. Even though some differences between estimated and experimental tail contribution were indicated, it is believed that the differences were not an appreciable part of the differences shown for the complete model.

CONCLUSIONS

An investigation at high subsonic speeds of the rolling stability derivatives of a complete general research model having an aspect-ratio-3 clipped-delta wing and a high horizontal tail indicated the following conclusions:

1. Positive damping in roll was indicated for the model throughout the test Mach number and angle-of-attack range, although significant losses in damping occurred in going from moderate to high angles of attack.

2. Addition of the tail surfaces to the wing-fuselage configuration had little overall effect on the damping in roll and gave negative increments of yawing moment due to roll throughout the test angle-of-attack range above approximately 4°.

3. Estimates made at $M = 0.85$ indicated that the rolling stability derivatives of the complete model could be estimated with fairly good accuracy by use of existing procedures.

4. Wing-fuselage damping-in-roll characteristics for the aspect-ratio-3 clipped-delta wing model were slightly better than the parent aspect-ratio-4 delta-wing model throughout the test Mach number range and angle of attack.

Langley Aeronautical Laboratory,
National Advisory Committee for Aeronautics,
Langley Field, Va., November 3, 1955.

REFERENCES

1. Wiggins, James W.: Wind-Tunnel Investigation of Effect of Sweep on Rolling Derivatives at Angles of Attack Up to 13° and at High Subsonic Mach Numbers, Including a Semiempirical Method of Estimating the Rolling Derivatives. NACA RM L54C26, 1954.

2. Wiggins, James W.: Wind-Tunnel Investigation at High Subsonic Speeds To Determine the Rolling Derivatives of Two Wing-Fuselage Combinations Having Triangular Wings, Including a Semiempirical Method of Estimating the Rolling Derivatives. NACA RM L53L18a, 1954.

3. Sleeman, William C., Jr.: Experimental Investigation at High Subsonic Speeds To Determine the Rolling-Stability Derivatives of Three Wing-Fuselage Configurations. NACA RM L54H11, 1954.

4. Few, Albert G., Jr.: Investigation at High Subsonic Speeds of the Static Longitudinal Stability Characteristics of a Model Having Cropped-Delta and Unswept Wing Plan Forms and Several Tail Configurations. NACA RM L55I23a, 1955.

5. Kuhn, Richard E., and Wiggins, James W.: Wind-Tunnel Investigation To Determine the Aerodynamic Characteristics in Steady Roll of a Model at High Subsonic Speeds. NACA RM L52K24, 1953.

6. Sleeman, William C., Jr., and Wiggins, James W.: Experimental Investigation at High Subsonic Speeds of the Rolling Stability Derivatives of a Complete Model With an Aspect-Ratio-2.53 Wing Having an Unswept 72-Percent-Chord Line and a High Horizontal Tail. NACA RM L54I20, 1955.

7. Gillis, Clarence L., Polhamus, Edward C., and Gray, Joseph L., Jr.: Charts for Determining Jet-Boundary Corrections for Complete Models in 7- by 10-Foot Closed Rectangular Wind Tunnels. NACA WR L-123, 1945. (Formerly NACA ARR L5G31.)

8. Herriot, John G.: Blockage Corrections for Three-Dimensional-Flow Closed-Throat Wind Tunnels, With Consideration of the Effect of Compressibility. NACA Rep. 995, 1950. (Supersedes NACA RM A7B28.)

9. Michael, William H., Jr.: Analysis of the Effects of Wing Interference on the Tail Contributions to the Rolling Derivatives. NACA Rep. 1086, 1952. (Supersedes NACA TN 2332.)

10. Goodman, Alex, and Thomas, David F., Jr.: Effects of Wing Position and Fuselage Size on the Low-Speed Static and Rolling Stability Characteristics of a Delta-Wing Model. NACA TN 3063, 1954.

11. Bird, John D.: Some Theoretical Low-Speed Span Loading Characteristics of Swept Wings in Roll and Sideslip. NACA Rep. 969, 1950. (Supersedes NACA TN 1839.)

12. Jaquet, Byron M., and Brewer, Jack D.: Low-Speed Static-Stability and Rolling Characteristics of Low-Aspect-Ratio Wings of Triangular and Modified Triangular Plan Forms. NACA RM L8L29, 1949.

13. Goodman, Alex, and Adair, Glen H.: Estimation of the Damping in Roll of Wings Through the Normal Flight Range of Lift Coefficient. NACA TN 1924, 1949.

14. Fisher, Lewis R.: Approximate Corrections for the Effects of Compressibility on the Subsonic Stability Derivatives of Swept Wings. NACA TN 1854, 1949.

15. Toll, Thomas A., and Queijo, M. J.: Approximate Relations and Charts for Low-Speed Stability Derivatives of Swept Wings. NACA TN 1581, 1948.

16. Wolhart, Walter D.: Influence of Wing and Fuselage on the Vertical-Tail Contribution to the Low-Speed Rolling Derivatives of Midwing Airplane Models With 45° Sweptback Surfaces. NACA TN 2587, 1951.

TABLE I

PRINCIPAL GEOMETRIC CHARACTERISTICS OF THE MODEL

Wing:	
Span, ft	2.572
Root chord, ft	1.500
Tip chord, ft	0.214
Mean aerodynamic chord, ft	1.018
Area, sq ft	2.20
Aspect ratio	3.00
Taper ratio	0.143
Quarter-chord sweep, deg	36.85
Airfoil section	NACA 65A006
Horizontal tail:	
Span, ft	1.162
Root chord, ft	0.581
Tip chord, ft	0
Mean aerodynamic chord, ft	0.388
Area, sq ft	0.337
Aspect ratio	4.00
Taper ratio	0
Quarter-chord sweep, deg	36.85
Airfoil section	NACA 65A006
Vertical tail:	
Span (measured from root chord), ft	0.683
Root chord (located 0.154 foot above fuselage center line), ft	0.912
Tip chord, ft	0.420
Mean aerodynamic chord, ft	0.696
Area, sq ft	0.454
Aspect ratio	1.02
Taper ratio	0.46
Quarter-chord sweep, deg	28.00
Airfoil section	NACA 65A006

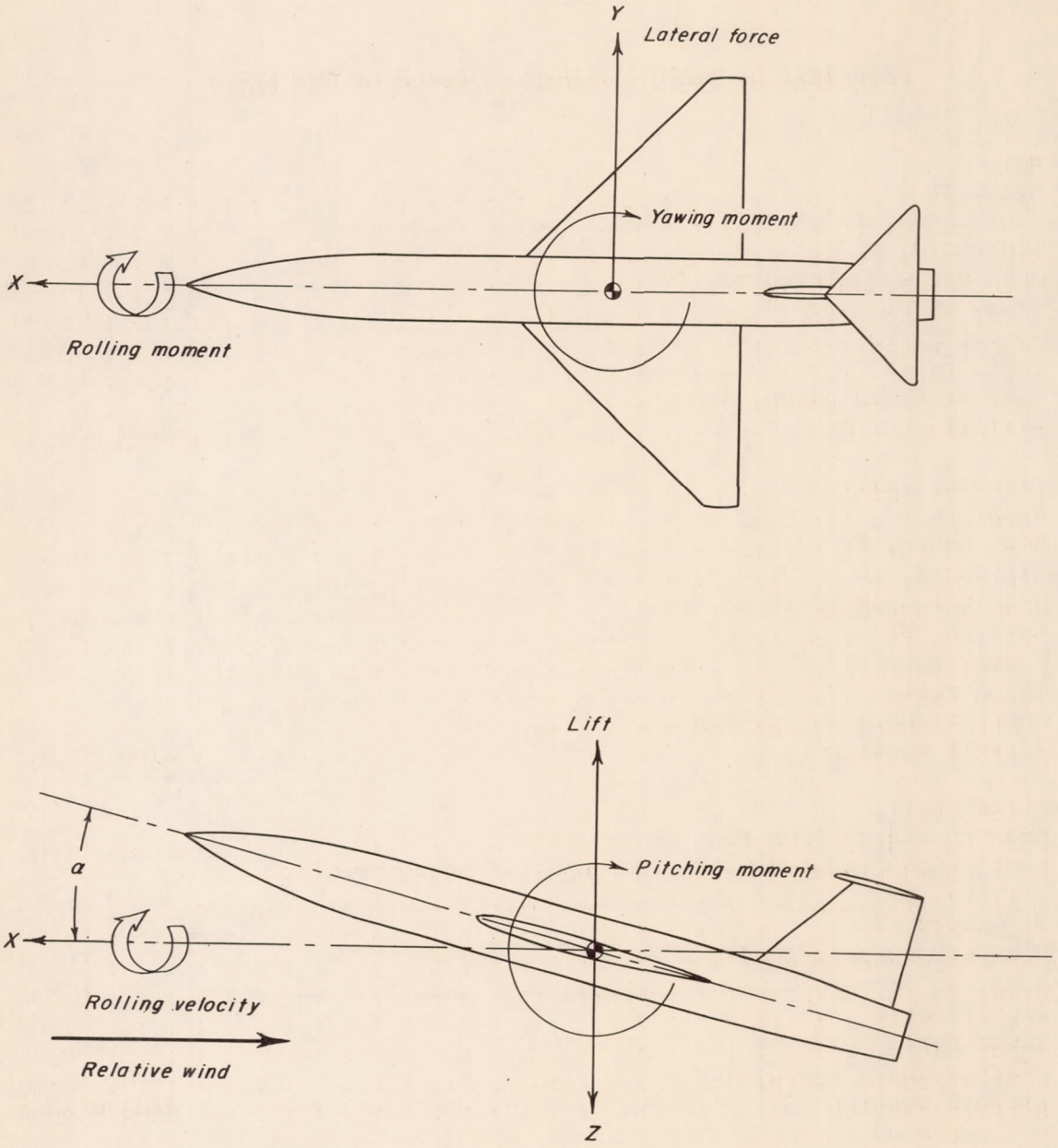


Figure 1.- Stability system of axes used showing positive directions of forces, moments, angles, and velocities.

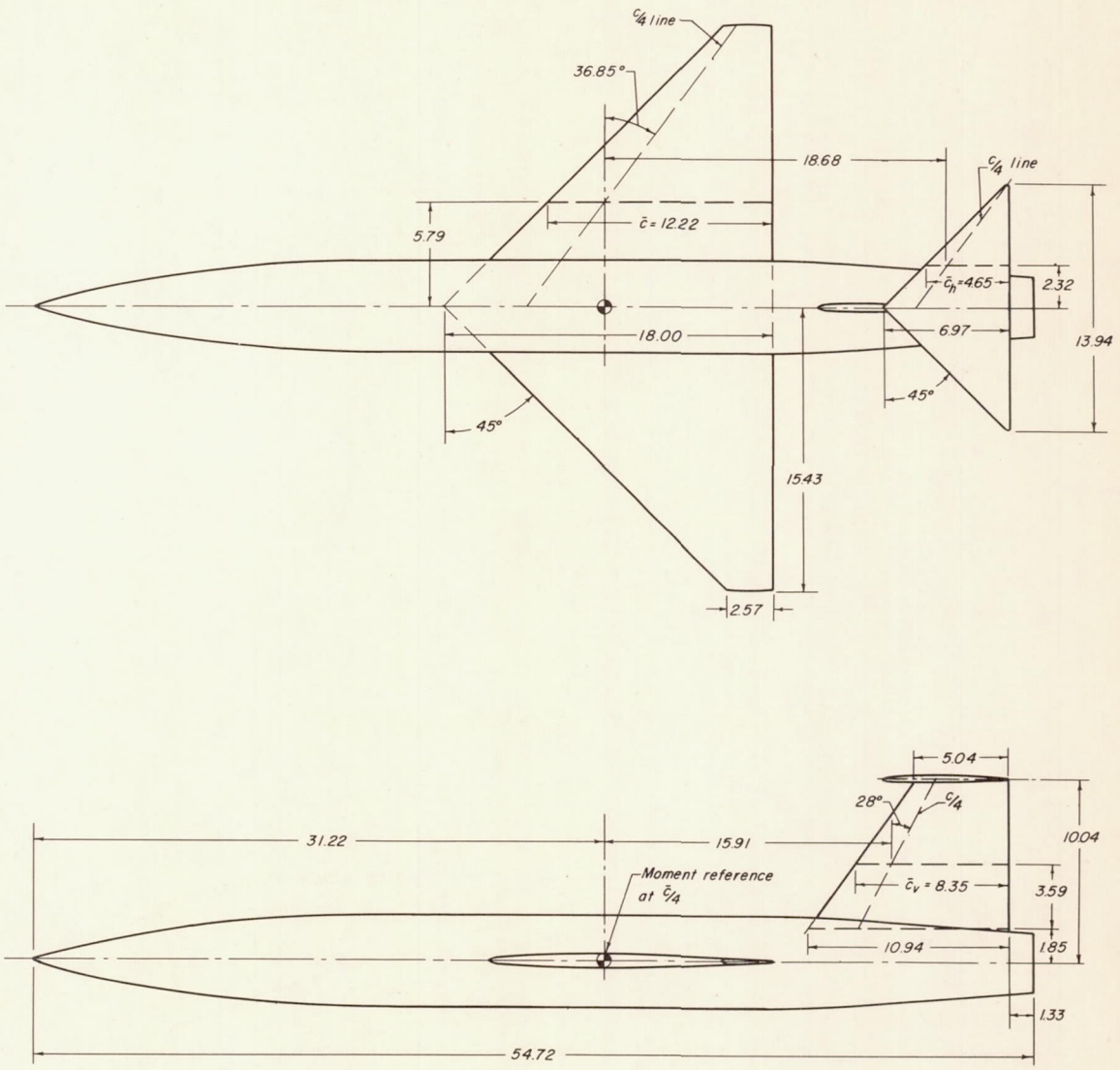
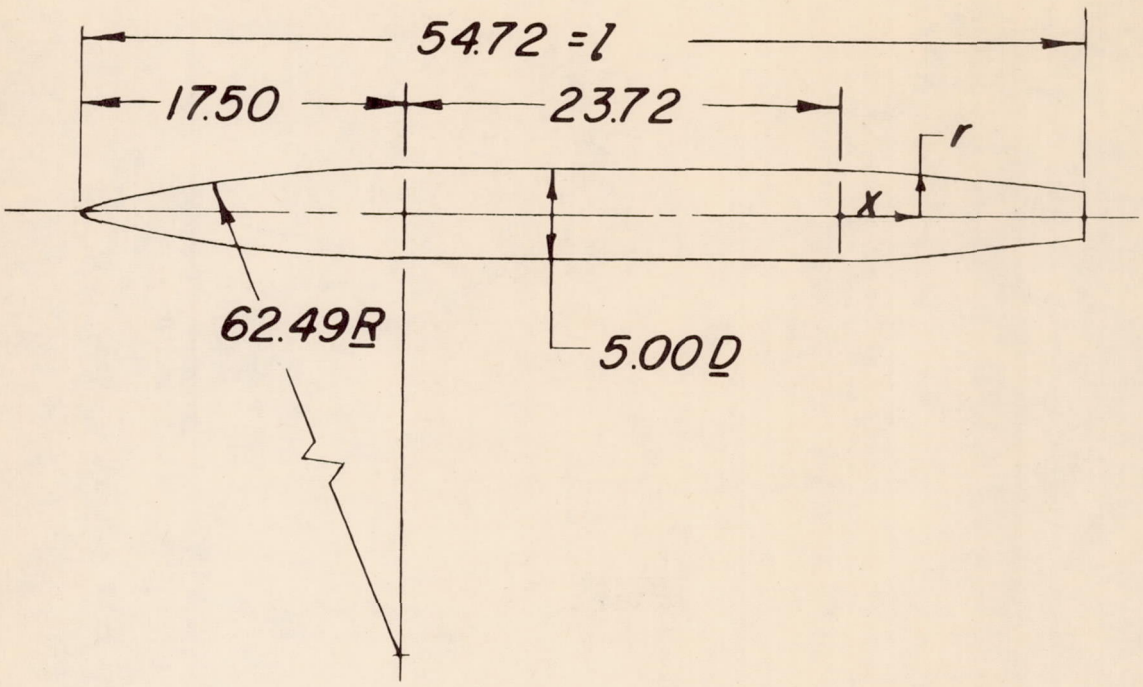


Figure 2.- General arrangement of the complete model tested in the Langley high-speed 7- by 10-foot tunnel. All dimensions are in inches.



Afterbody Coordinates

x/l	r/l
0	.0456
.0320	.0445
.0639	.0427
.1187	.0390
Straight-line taper	
.2460	.0301

Figure 3.- Geometric characteristics of the model fuselage. All dimensions are in inches.

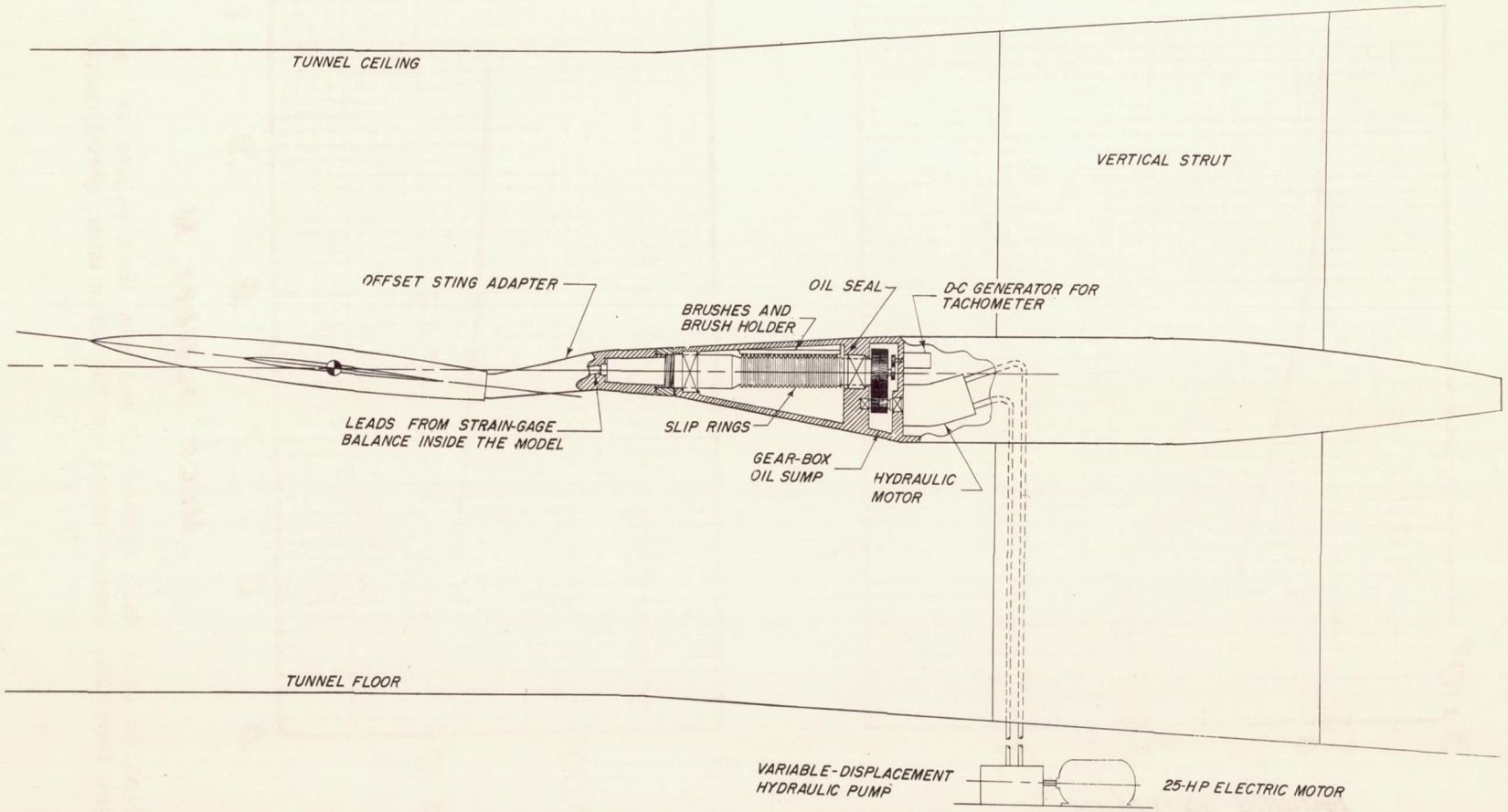


Figure 4.- General arrangement of the forced-roll support system.

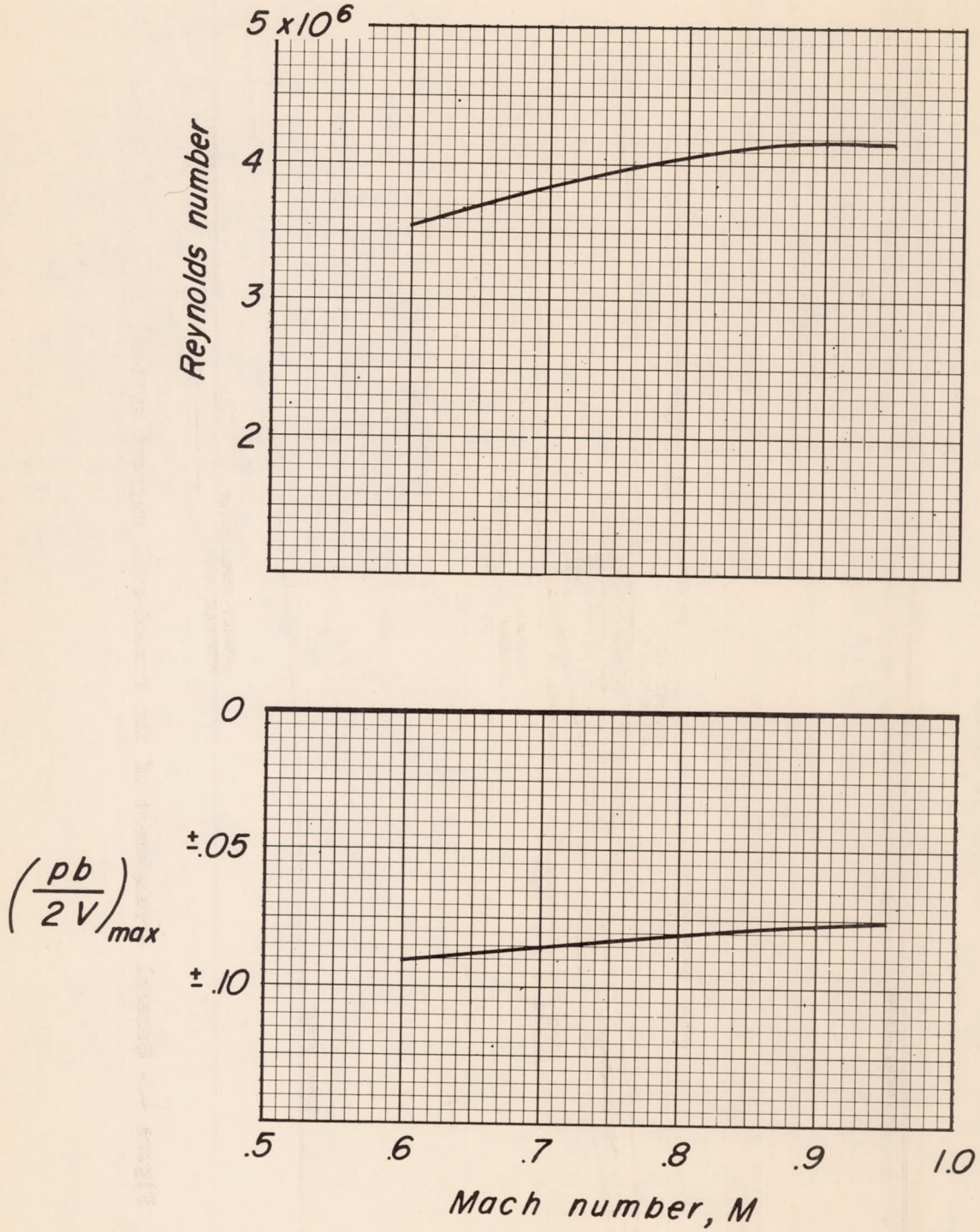


Figure 5.- Variation with Mach number of maximum test values of pb/2V and mean test Reynolds number based on the wing mean aerodynamic chord.

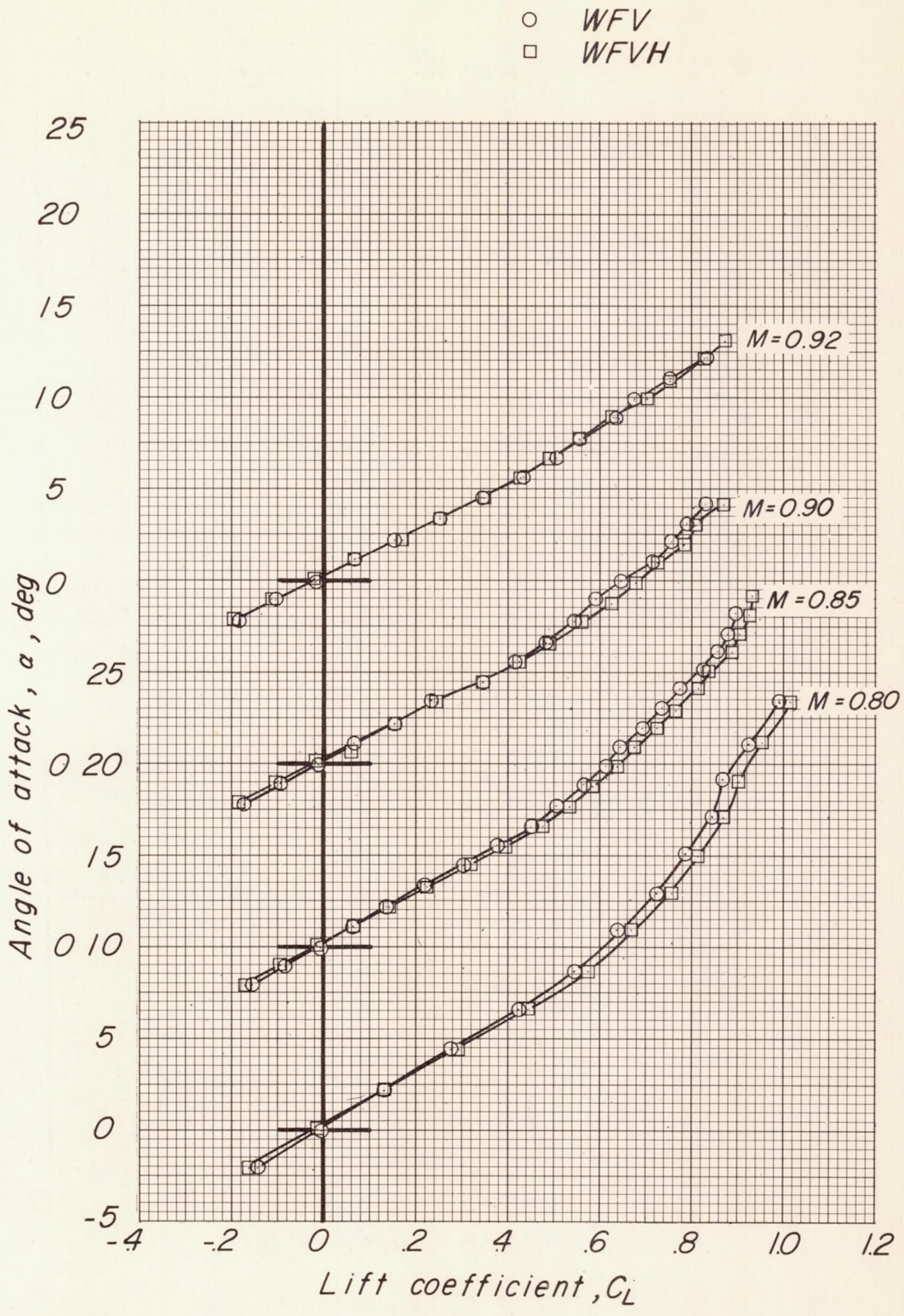


Figure 6.- Variation of lift coefficient with angle of attack obtained from reference 4.

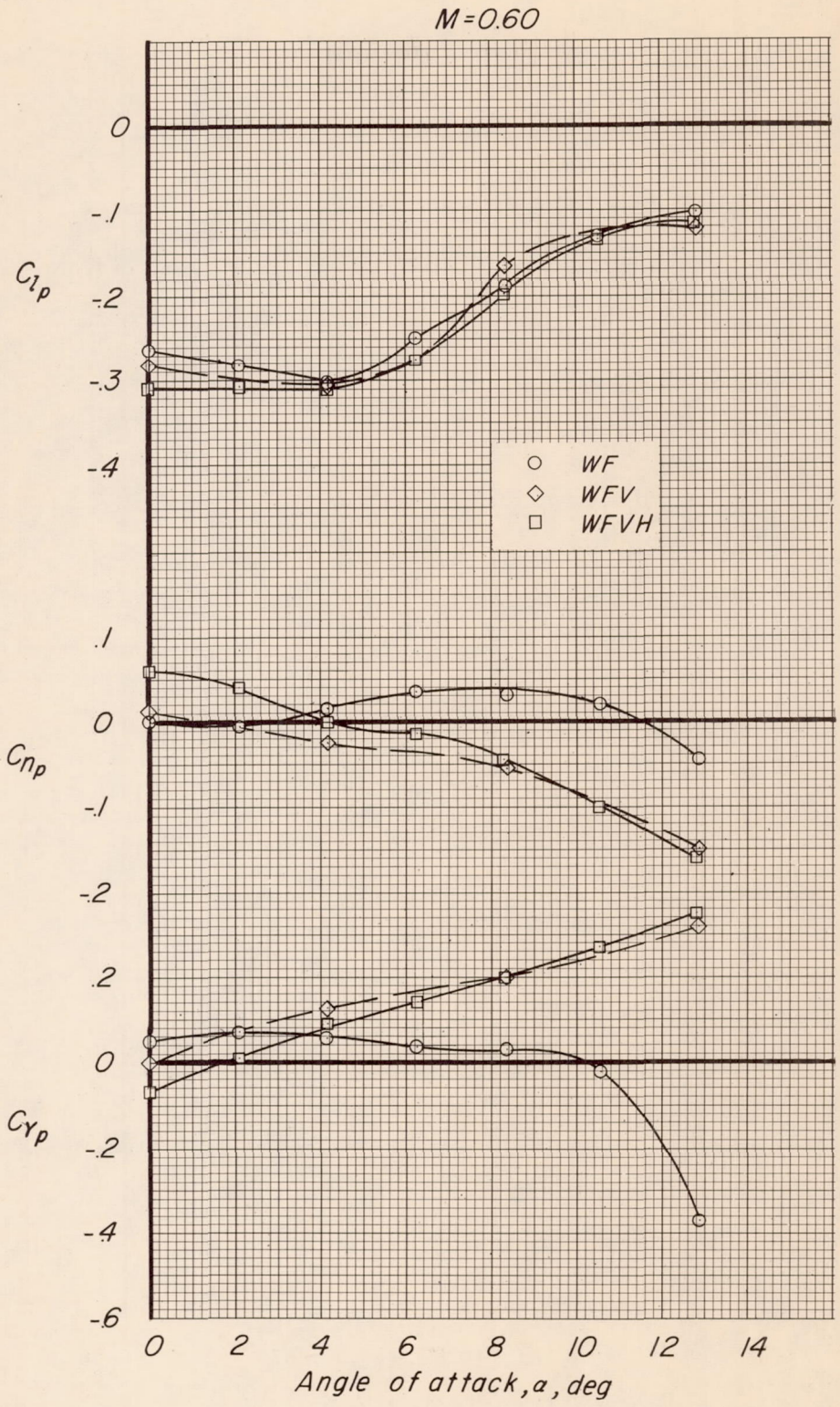


Figure 7.- Variation of rolling stability derivatives with angle of attack for the complete model, showing effects of the tail surfaces.

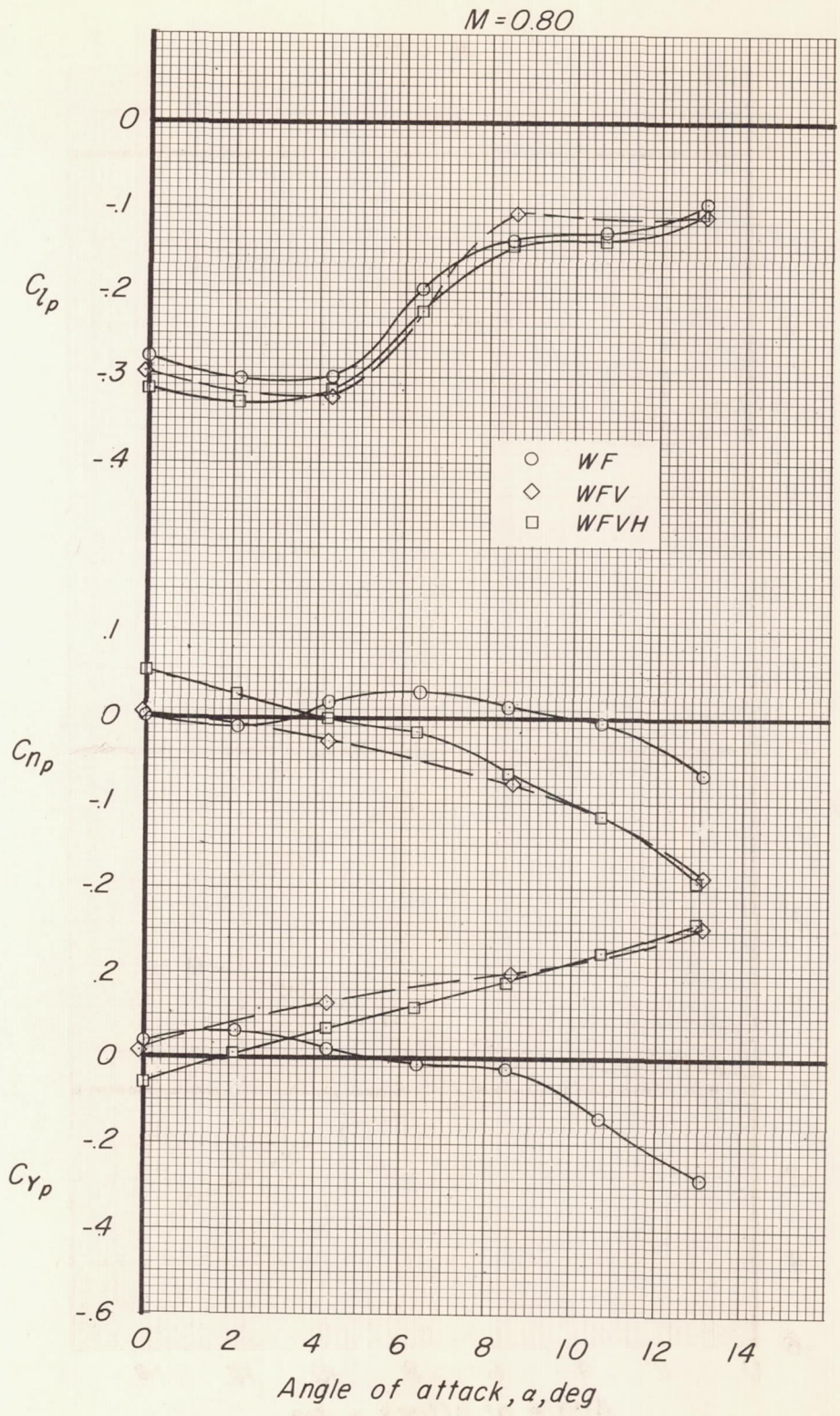


Figure 7.- Continued.

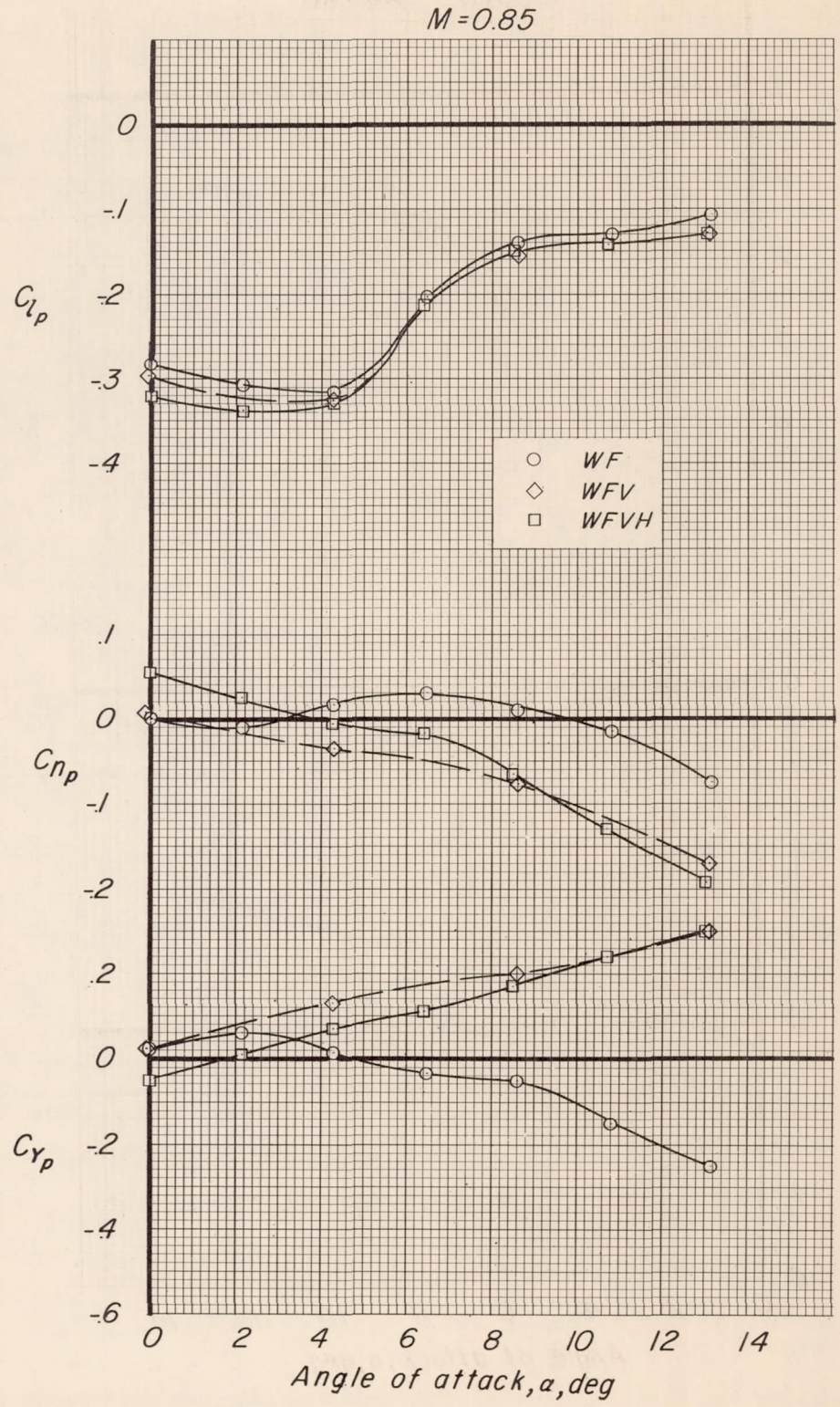


Figure 7.- Continued.

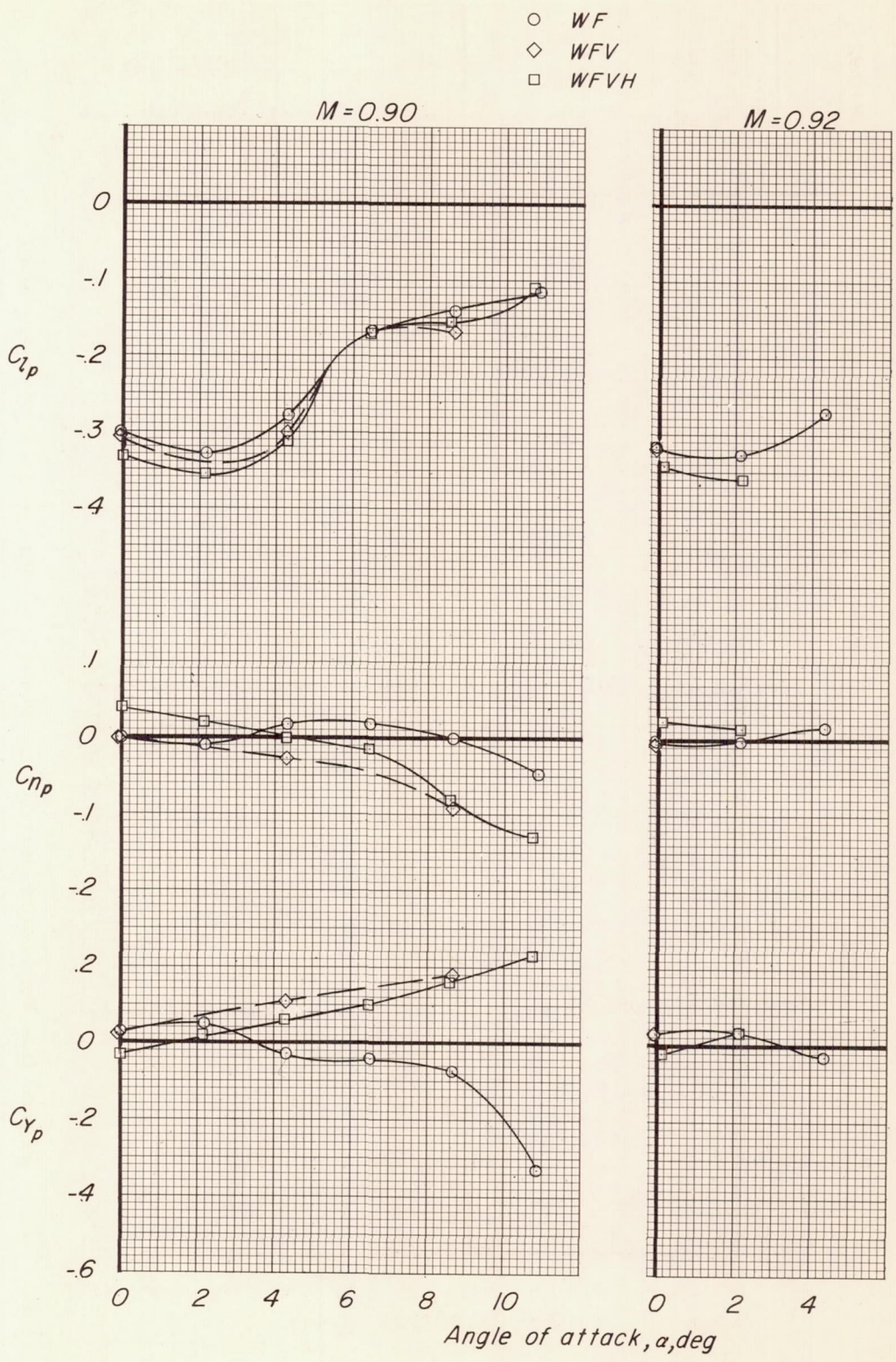


Figure 7.- Concluded.

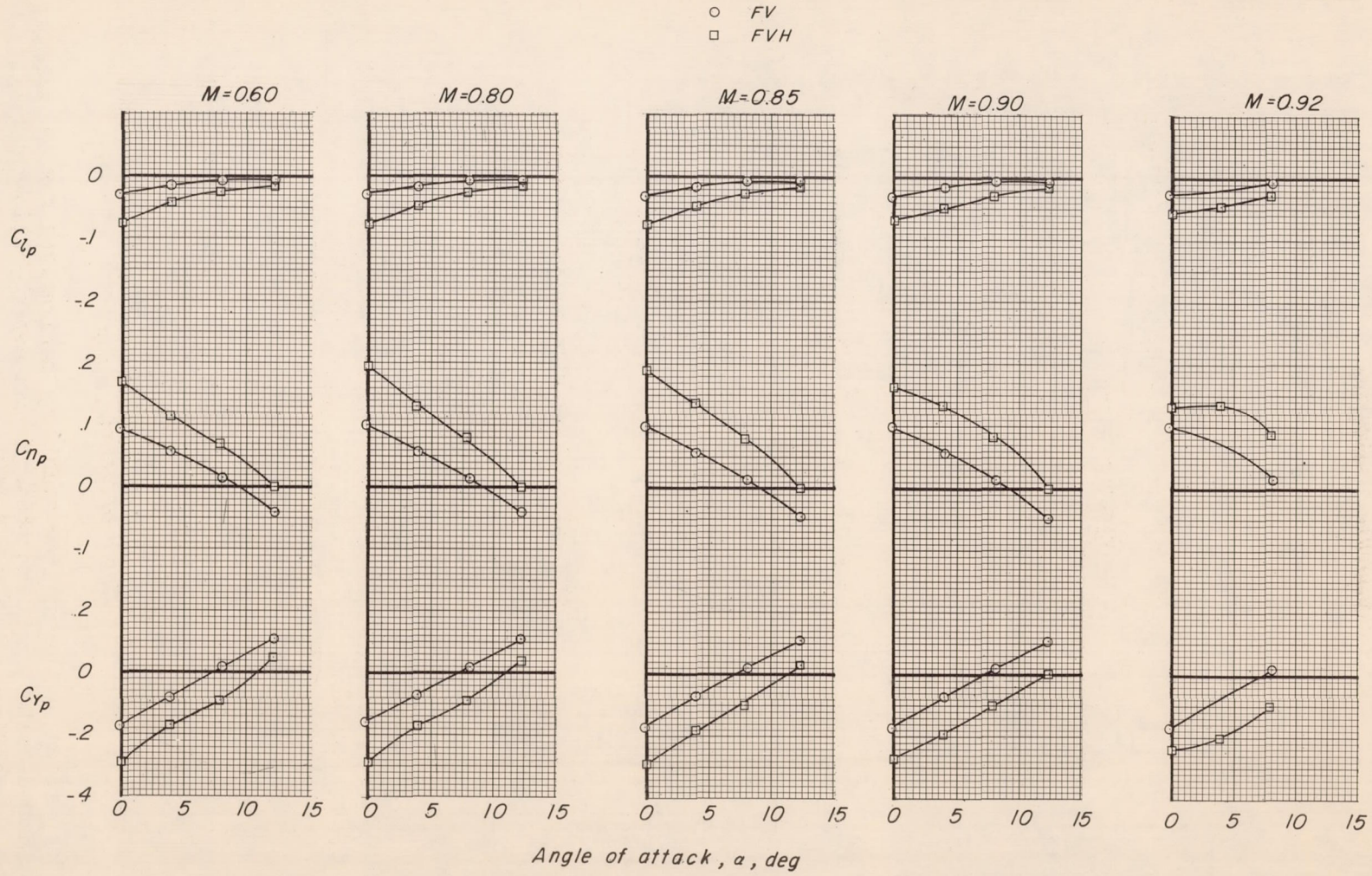


Figure 8.- Variation of rolling stability derivatives with angle of attack for the model without the wing, showing effects of the horizontal tail.

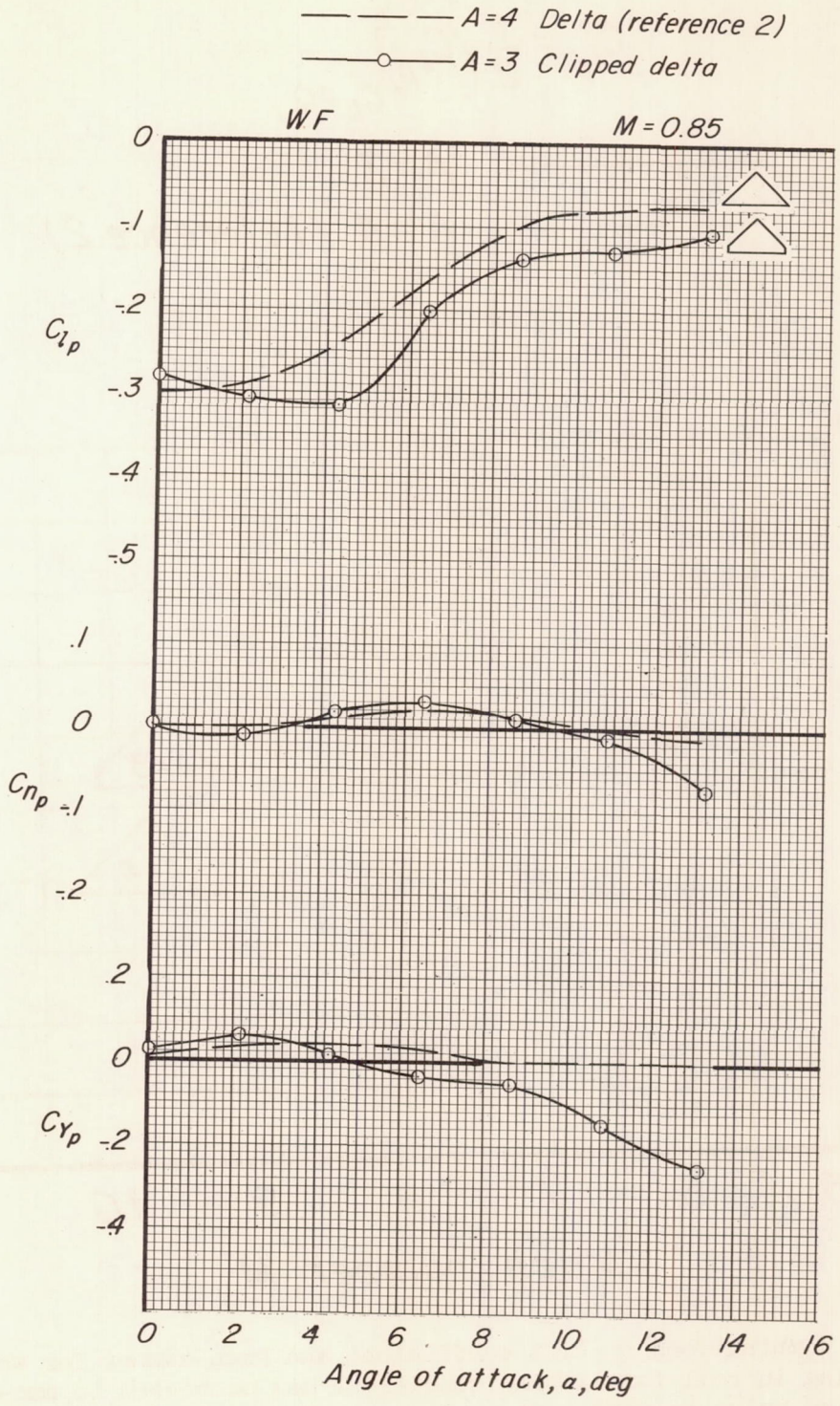


Figure 9.- Comparison of the rolling stability derivatives for the aspect-ratio-3 clipped-delta wing with those for an aspect-ratio-4 delta wing. Wing-fuselage configuration; M = 0.85.

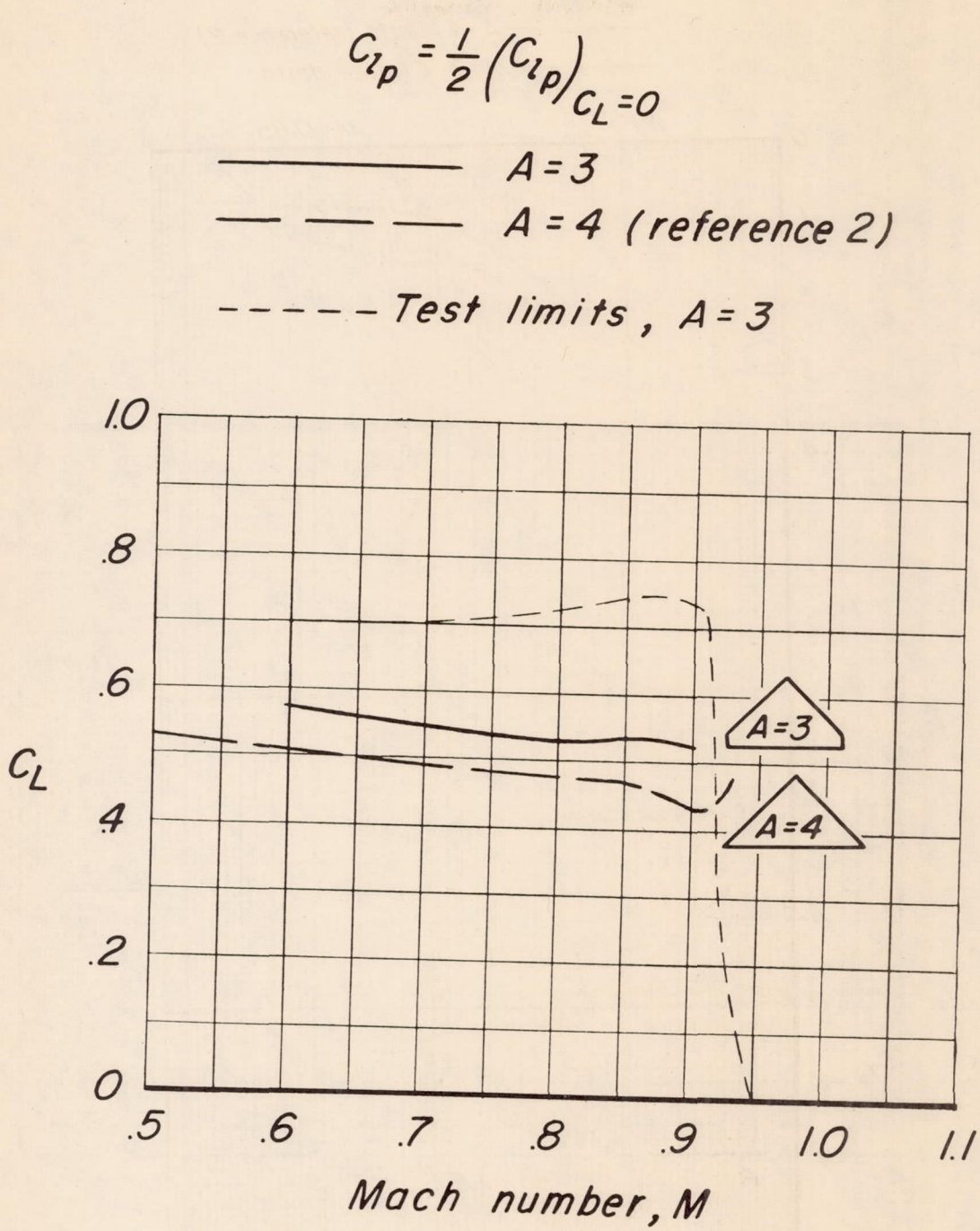


Figure 10.- Combinations of lift coefficient and Mach number for which the damping in roll for lifting conditions has decreased to one-half the damping value at zero lift.

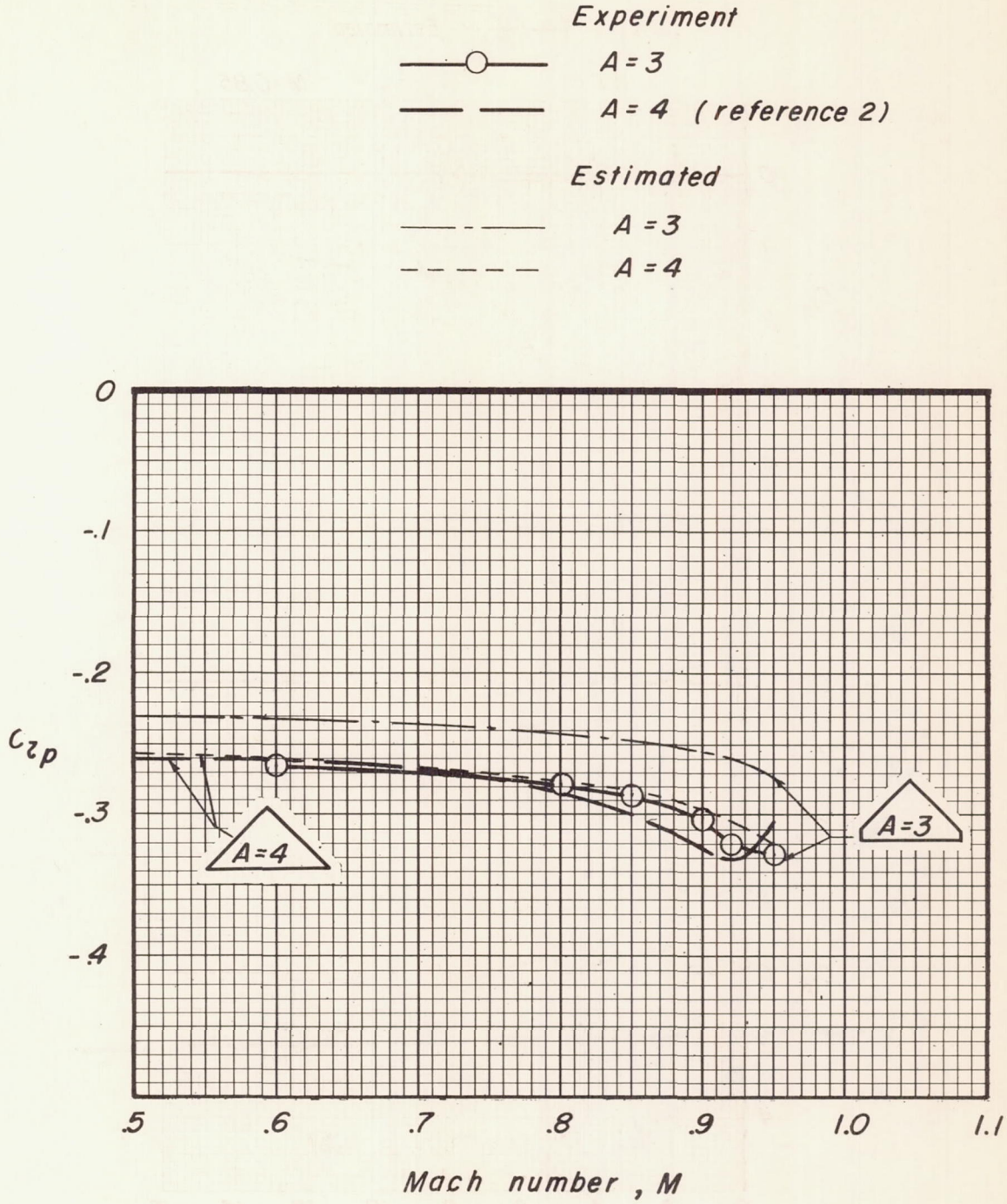


Figure 11.- Comparison of estimated and experimental damping in roll at zero lift for the aspect-ratio-3 clipped-delta model and the aspect-ratio-4 delta wing model; wing-fuselage configuration.

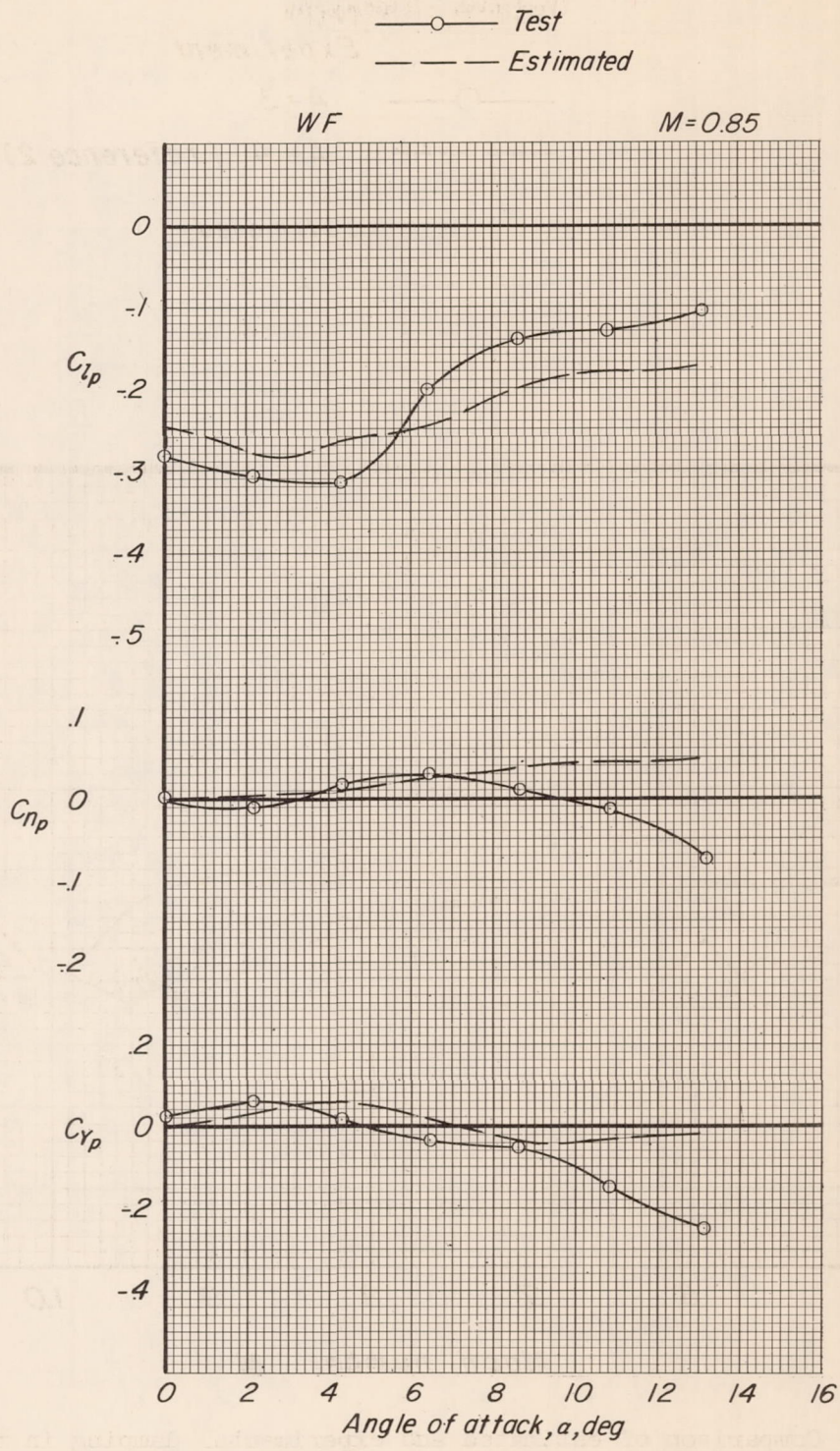


Figure 12.- Comparison of estimated and experimental rolling stability derivatives through the angle-of-attack range for the wing-fuselage configuration; M = 0.85.

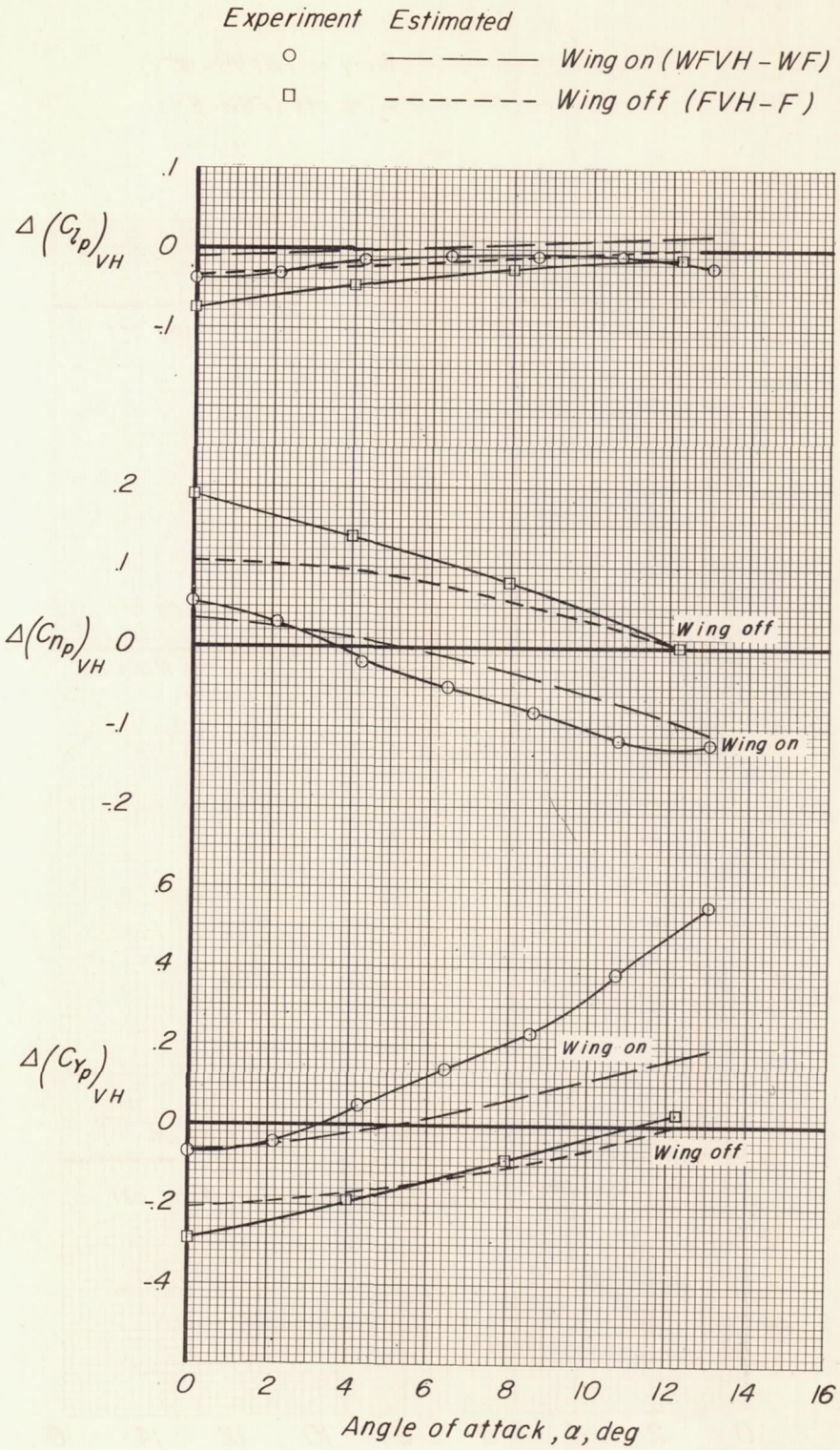


Figure 13.- Estimated and experimental tail contribution to rolling stability derivatives; M = 0.85.

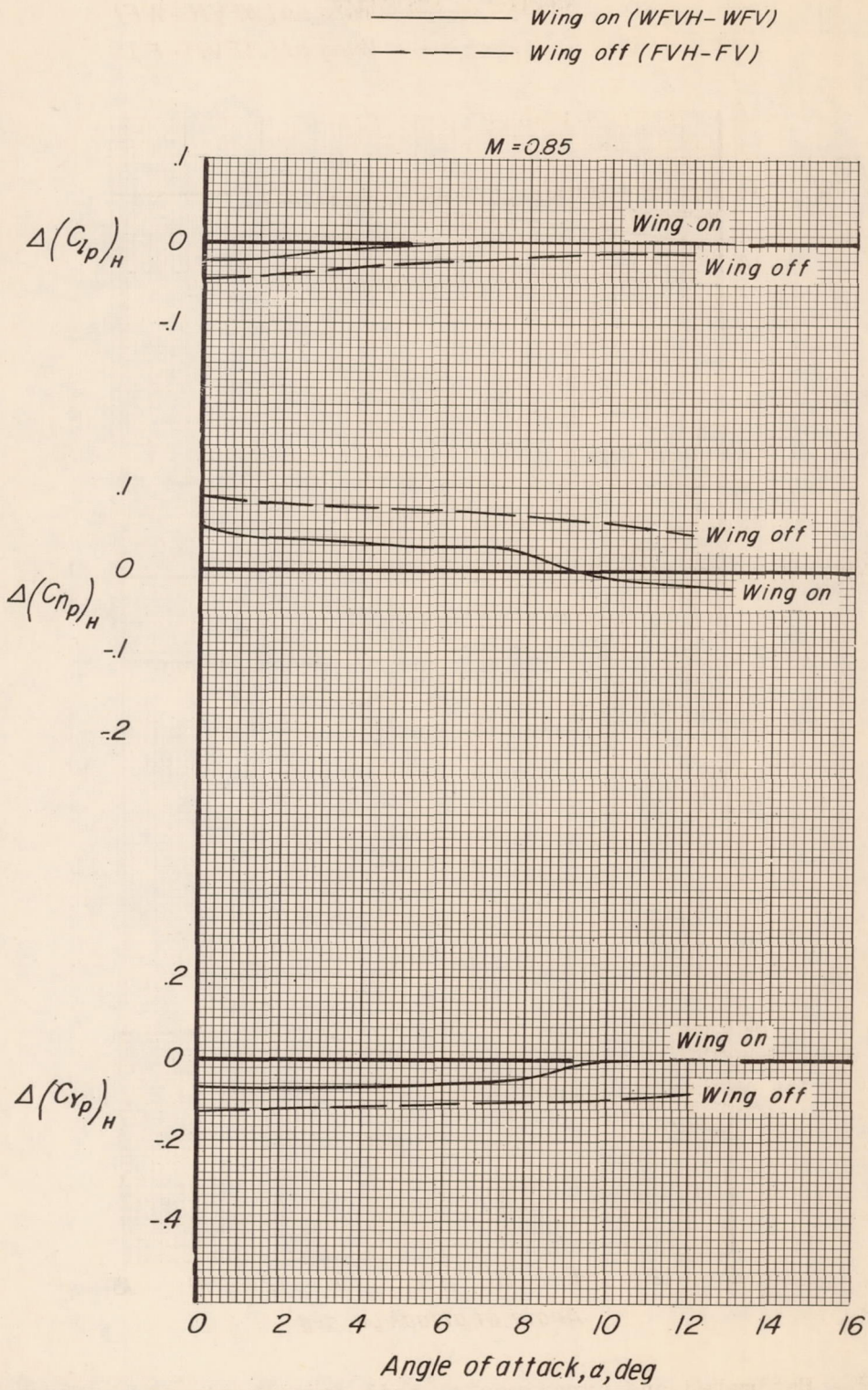


Figure 14.- Effect of the horizontal tail on rolling stability derivatives as determined from experiment; M = 0.85.

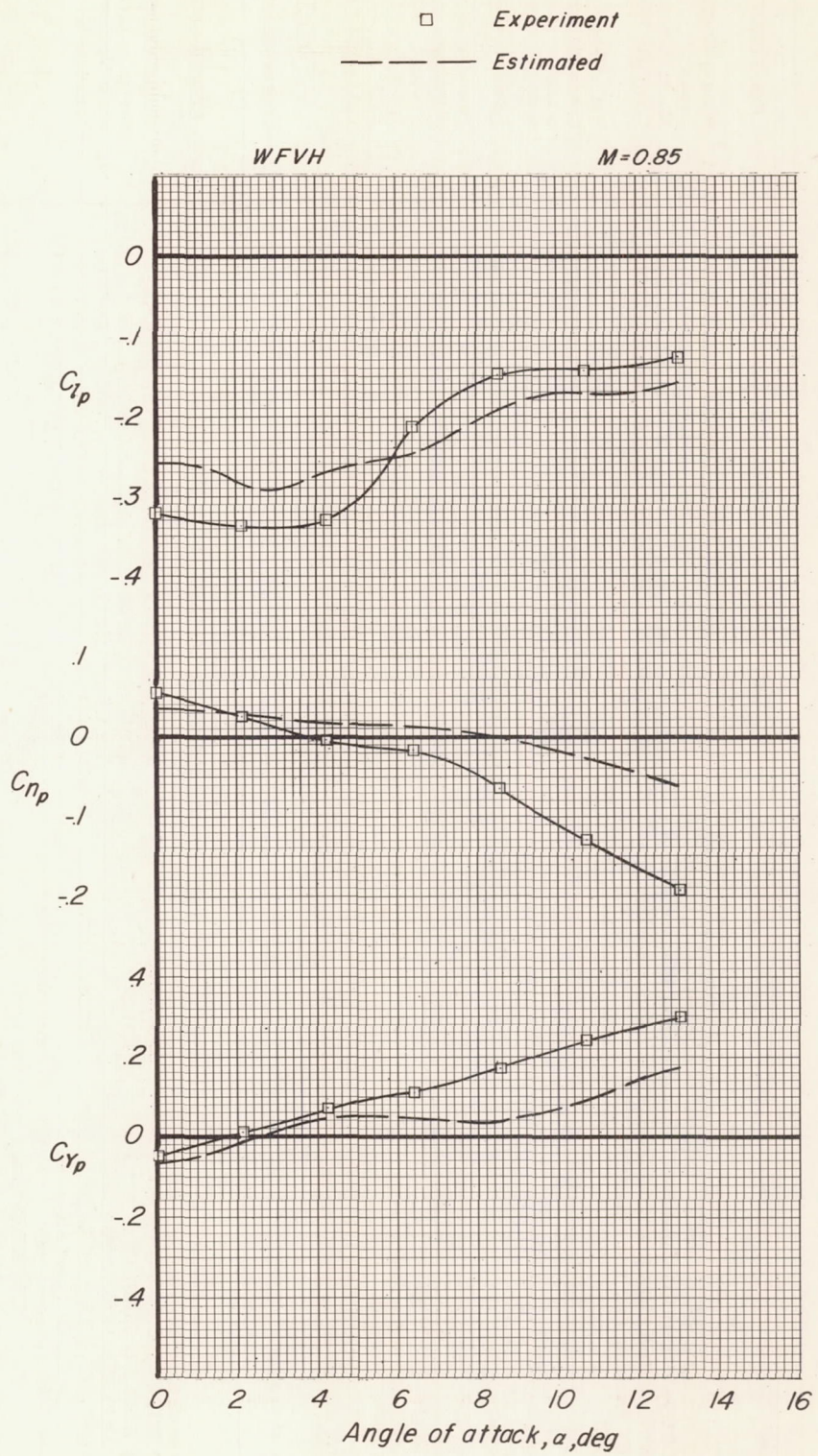


Figure 15.- Comparison of estimated and experimental rolling stability derivatives for the complete-model configuration; M = 0.85.

NACA - Langley Field, Va.